JARO 5: 295–304 (2004)
DOI: 10.1007/s10162-004-4044-3

JARO
Journal of the Association for Research in Otolaryngology

A Comparative Study of Eya1 and Eya4 Protein Function and Its Implication in Branchio-oto-renal Syndrome and DFNA10

YUZHOU ZHANG,[1] BOYD M. KNOSP,[2] MARK MACONOCHIE,[3] RICK A. FRIEDMAN,[4] RICHARD J.H. SMITH[1]

[1]*Molecular Otolaryngology Research Laboratories, University of Iowa, Iowa City, IA 52242, USA*
[2]*The University of Iowa ITS Research Service, University of Iowa, Iowa City, IA 52242, USA*
[3]*School of Life Sciences, University of Sussex, Falmer, Brighton, BN1 9QG, UK*
[4]*House Ear Institute, Los Angeles, CA 90057, USA*

Received: 24 October 2003; Accepted: 29 March 2004; Online publication: 30 July 2004

ABSTRACT

Allele variants of *EYA1* and *EYA4*, two members of the vertebrate *Eya* gene family, underlie two types of inherited human deafness, branchio-oto-renal (BOR) syndrome and DFNA10, respectively. To clarify how mutations in these two genes and their encoded proteins impact the normal biology of hearing, we completed a number of functional studies using the yeast-two-hybrid system. We verified that bait constructs of the homologous region (*Eya1HR* and *Eya4HR*) interact with *Six1* prey constructs, although no interaction with *Dach1* prey was demonstrable. To compare interaction affinities, we evaluated α-galactosidase activity after cotransformation of *Eya1HR/Six1* and *Eya4HR/Six1* and found that the latter interaction was weaker. By immunofluorescence staining, we showed Eya4HR localization to the cytoplasm. After coexpression of *Six1*, Eya4HR was translocated to the nucleus. Results with Eya1HR were similar. Translation of mutant constructs ($Eya4HR_{R564X}$ and $Eya1HR_{R539X}$) could not be demonstrated. Using dual *Eya*-containing constructs (with two wild-type alleles or wild-type and mutant alleles), we confirmed no translation of the mutant allele, even if the mutation was nontruncating. These results are consistent with clinical data and implicate haploinsufficiency as the cause of BOR syndrome and DFNA10.

Keywords: *Eya* gene family, *Six* gene family, branchio-oto-renal syndrome, DFNA10, haploinsufficiency

INTRODUCTION

The vertebrate *Eya* gene family is comprised of four transcriptional activators that interact with other proteins in a conserved regulatory hierarchy to ensure normal embryologic development. The structure of these proteins as deduced from their cDNA sequences includes a highly conserved 271-amino acid carboxy terminus called the eya-homologous region (eyaHR) and a more divergent proline–serine–threonine (PST)-rich (34%–41%) transactivation domain at the amino terminus (eya variable region, eyaVR) (Zimmerman et al. 1997) (Fig. 1). Studies in *Drosophila* indicate that the eyaHR mediates interactions with the gene products of *so* (sine oculis) and *dac* (dachshund), and that expression of both *eya* and *so* is initiated by *ey* (eyeless) (Bonini et al. 1993, 1997; Pignoni et al. 1997). The vertebrate orthologs of *so* are members of the *Six* gene family and similarly bind with Eya proteins, inducing nuclear translocation of the resultant protein complex (Ohto et al. 1999). Amino terminal transcriptional activation also has been demonstrated for the *Drosophila eya* and murine

Correspondence to: Richard J.H. Smith • Department of Otolaryngology • University of Iowa • 200 Hawkins Drive • Iowa City, IA 52242. Telephone: (319) 356-3612; fax: (319) 356-4547; email: richard-smith@uiowa.edu

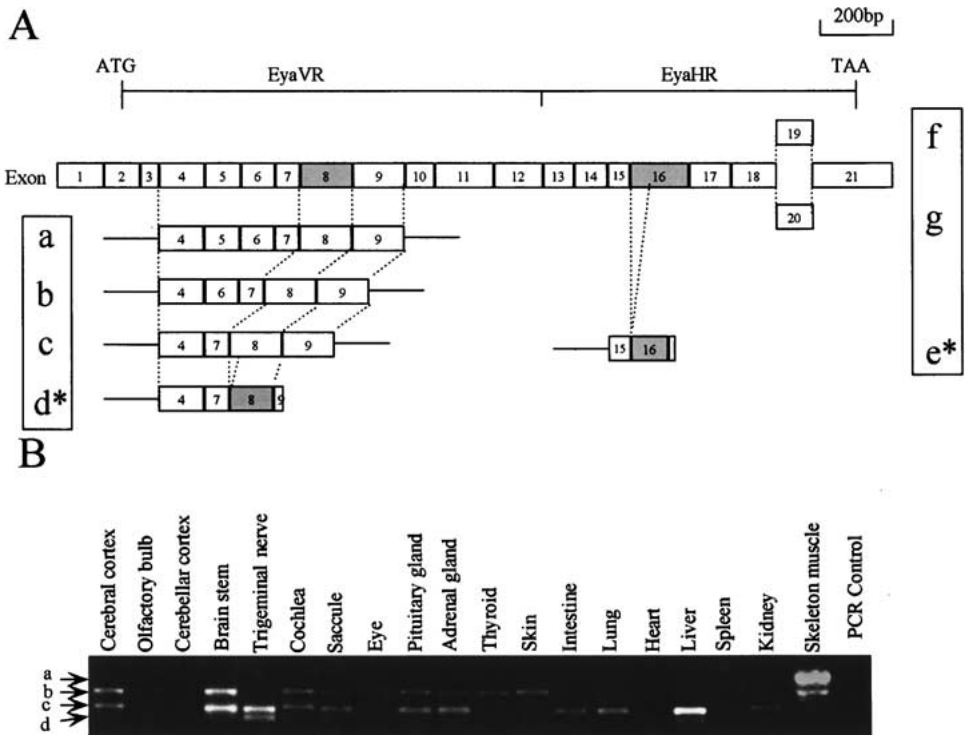

FIG. 1. Schematic illustrating the structure of the Eya4 protein showing its EyaVR and EyaHR domains. In embryonic tissue, all EyaVR isoforms (a,b,c) are associated with EyaHR isoform f and occasionally isoform e; in adult tissue, all EyaVR isoforms (a,b,c) are associated with EyaHR isoform g. Isoform d lacks the 5′ 28 base pairs of exon 8, and encodes a putative protein that lacks the EyaHR (**A**). Expression profiles are tissue specific (**B**). VR, variable region; HR, homologous region.

Eya1–3 gene products, an additional indication that *Eya* interactions and pathways are conserved across species (Pignoni et al. 1997; Xu et al. 1997).

Expression of *Eya* genes is present in a wide variety of tissues early in embryogenesis, and although each gene has a unique expression pattern there is extensive overlap. For example, murine studies have shown that *Eya1, Eya2,* and *Eya4* are all expressed in the presomitic mesoderm and head mesenchyme, but only *Eya1* and *Eya4* are expressed in the otic vesicle (Ohto et al. 1999). *Eya3* expression is restricted to craniofacial and branchial arch mesenchyme in regions underlying or surrounding the Eya1-, 2-, or 4-expressing cranial placodes (Heanue et al. 1999).

Allele variants of *EYA1* and *EYA4* underlie two types of inherited human deafness, branchio-oto-renal (BOR) syndrome (Abdelhak et al. 1997b) and DFNA10 (Wayne et al. 2001), respectively. The clinical phenotype in persons with BOR syndrome is characterized by numerous congenital anomalies involving the branchial arch system, inner and middle ears, and kidneys, with the most common features being deafness (98.5%), preauricular pits (83.6%), branchial anomalies (68.5%), renal anomalies (38.2%), and external ear abnormalities (31.5%) (Chen et al. 1995). In persons with DFNA10, there are no abnormalities aside from late-onset hearing loss (De Leenheer et al. 2001).

These phenotypic differences are surprising given the expression profiles of *EYA1* and *EYA4* in embryogenesis. Both genes are expressed early in the otic vesicle in rodent inner ears, although *in situ* hybridization studies we have done show a spatial variability in *Eya4* expression that is not seen with *Eya1* expression (Wayne et al. 2001). After the otic vesicle differentiates into auditory and vestibular components, *Eya4* becomes concentrated in cells of the upper cochlear duct destined to develop into the stria vascularis and Reissner's membrane, while *Eya1* is expressed in the floor of the cochlear duct in an area that gives rise to the organ of Corti. Throughout development, *Eya1* expression is maintained in derivatives of the neuroepithelium of the cochlear duct floor, while *Eya4* expression shifts only from the upper cochlear duct to the neuroepithelium of the cochlear duct floor at embryonic day 18.5 (E18.5) (Wayne et al. 2001).

These data suggest a disjunct between the expression pattern of *Eya4* and the DFNA10 phenotype. Since there is overlap in expression of *Eya1* and *Eya4* during embryogenesis, this disjunct may reflect functional redundancy of *Eya4* to *Eya1* in develop-

TABLE 1

Primers for *Eya* constructs

	Forward	*Reverse*	*Amino acid sites*
Eya4FR	cgatcatatgtggcagtggcaagagaagt (N)	attcgtcgacacaatggatccccagctaga (S)	1–616
Eya4VL	cgatcatatgtggcagtggcaagagaagt (N)	ctatgtcgaccggaggtggggagagatta (S)	1–341
Eya4HR	Caatcatatgagaagttctgggtcaaagtctcg (N)	ctatgaattcacaatggatccccagctaga (E)	322–616
Eya1HR	cgatcatatgcgaggttcagatgggaagtc (N)	tgatgaattccagtgtcaagttggcaggaa (E)	296–591
Eya4HR1	Caatcatatgagaagttctgggtcaaagtctcg (N)	actcgaattccaaacaaaggttcgcacta (E)	322–444
Eya4HR2	cagtcatatgctccggatggaagaaatgat (N)	actagaattcgaatcagctgggttgtcgtt (E)	384–530
Eya4HR3	tcgatcatatggcagagatcgaaggcctaac (N)	ctatgaattcacaatggatccccagctaga (E)	493–616
Eya4HR4	Caatcatatgagaagttctgggtcaaagtctcg (N)	actagaattcgaatcagctgggttgtcgtt (E)	322–530
Eya4HR5	cagtcatatgctccggatggaagaaatgat (N)	ctatgaattcacaatggatccccagctaga (E)	384–616
Eya4HR6	Eya4HR1+Eya4HR3		Del 49aa (444–493)

A restriction enzyme site (underlined) was added to the 5′ flank of each primer. N = *Nde*I, E = *Eco*RI, S = *Sal*I

ment but not in the mature organ system. In this article, we compare the function of *Eya1* and *Eya4* to clarify how mutations in these two genes and their encoded proteins impact the normal biology of hearing and result in BOR syndrome and DFNA10, respectively.

MATERIALS AND METHODS

Expression profiling

To determine whether novel isoforms of *Eya4* exist, expression studies were performed against a panel of cDNA from different tissues using two sets of primers: Set 1 for detecting variants in *Eya4VR* (AF in exon 4,5'-TGGTTGGAGGCAGTGATACA-3'; AR in exon 9,5'-TGGCAACATCACACCAAGAT-3') and Set 2 for detecting variants in *Eya4HR* (BF in exon 13, 5'-AACGACAACCCAGCTGATTC-3'; BR_{ex19} in exon 19, 5'-GGTTAGCAGCGTGCTCCTCA-3'; and BR_{ex20} in exon 20, 5'-TTTTTGCTGCCTGCTCTTCT-3').

Expression constructs

To subclone *Eya*, total RNAwas isolated from E11 mouse embryos and skeleton muscle using the Rneasy protocol (Qiagen, Northridge, CA). Five micrograms were reverse transcribed into cDNA in a final volume of 20 μl using Superscript III (Invitrogen, Carlsbad, CA) before amplifying with the following primer pairs, each designed to include restriction endonuclease sites at their 5' ends: *Eya4VR*, $Eya4HR_{ex19}$ (*Eya4HR* with the exon 19 splice variant), $Eya4HR_{ex20}$ (*Eya4HR* with the exon 20 splice variant), *EYa4FL* (full length –*eyaVR* and *eyaHR*), and *Eya1HR* (Table 1). For yeast-two-hybrid studies, these RT-PCR products were fused with the Gal-4 DNA-binding domain of pGBKT7 (bait). To identify the requisite portion of *Eya4* for interaction with Six1, we also generated several truncated forms of *Eya4HR* (Table 1, Fig. 2A). *Six1* and *Dach1* were rescued from *Six1*/RCAS and *Dach1*/pBS vectors and fused with the Gal-4 activation domain of pGADT7 (prey).

To construct mammalian expression plasmids, c-myc-tagged *Eya1HR* or *Eya4HR* was subcloned into pBudCE4.1 (Invitrogen, Carlsbad, CA) under control of the CMV promoter. HA-tagged *Six1* was inserted into another multicloning site of the same vector under control of the EF-1α promoter. Flag-tagged *Dach1* was subcloned into p3XFIag-CMV-10 vector (Sigma-Aldrich, St. Louis, MO).

Yeast-two-hybrid assays

The MATCHMAKER 3 Gal-4 Yeast-Two-Hybrid (Y2H) system (Clontech, Palo Alto, CA) was selected for yeast interaction assays and library screening. Co-transformations were completed using the lithium acetate method to introduce each of the pGBKT7 bait constructs and each of the pGADT7 prey constructs into yeast AH109.

Yeast mating library screening was performed by single lithium acetate transformation to introduce bait *Eya4HR* to yeast AH109 (mat a). Transformed AH109 was selected on synthetic dropout media lacking tryptophan before mating with pretransformed yeast Y187 (mat α) prey libraries derived from either mouse adult brain (Clontech, Palo Alto, CA) or mouse E10.5 otic vesicle. Mating cultures were selected on dropout media lacking tryptophan, leucine, histidine, and adenine, and containing 15 mM 3-amino-triazole.

To eliminate possible false positives, yeast plasmids were extracted using a modified Qiagen miniprep protocol (Singh and Weil 2002). Potential interacting preys were rescued by electroporating to DH5α competent cells on ampicillin medium. Rescued preys were reintroduced to AH109 with bait *Eya4HR* to

verify the bait–prey interaction. The reporter gene assays were completed by α-galactoside quantification as described by the manufacturer (Clontech, PaloAlto, CA).

Cell cultures and immunofluorescence staining

Human embryonic kidney (HEK) 293 cells and monkey kidney Cos-7 cells were maintained in DMEM (Gibco) supplemented with 4 mM L-glutamine and 10% fetal bovine serum (Hyclone, Logan, UT). For immunofluorescence staining, cells were transfected at 30%–50% confluency with Fugene™ (Roche Molecular Biochemicals, Indianapolis, IN) on 4-well Chamber Slides™ (Lab Tek, New Zealand), according to the manufacturer's instructions. After an incubation period of 24–48 h, transfected cells were fixed with –20°C methanol and permeablized with 0.1% Triton X-100 in PBS. The slides were blocked in 10% BSA overnight before incubating with 1:25 diluted anti-Myc (9E10: Santa Cruz Biotechnology, Santa Cruz, CA), anti-HA (Y–11; Santa Cruz Biotechnology), or anti-FLAG (Sigma-Aldrich) antibodies, as appropriate, in PBS with 3% BSA. Detection was achieved using a 1:200 dilution of bovine anti-mouse IgG and/or bovine anti-goat IgG conjugated with either FITC or Texas-red (Santa Cruz Biotechnology) in PBS with 3% BSA.

Mutagenesis

Eya1 or *Eya4* mutants that have been associated with human disease were generated by site-directed mutagenesis using the Quik™ Change protocol (Stratagene, La Jolla, CA). The forward primer and its complementary primer were used for each construct (mutagenized nucleotides are in upper case) *Eya1R539X* (ggaaagctgtttTgAgtgaataatccaaaggtttgg), *Eya4HRR564X* (gaaagttgctttgagTgaataatgcaaaggtttgg cag), *Eya1HRL504R* (gtaacaactacgcagcGcagcccag cattggc). Briefly, 10 ng plasmid DNA was used for PCR cycling in a 50-μl volume with pfu Turbo DNA polymerase containing 125 ng of each primer and 0.2 mM dNTPs. The mutated plasmid template was digested with Dpnl (10 U) to remove the parental strain and used to transform XL1-Blue competent cells. All mutant constructs were confirmed by sequencing.

Western blotting

Yeast lysates from transformed strain AH109 were extracted using glass beads in extraction buffer (200 mM Tris pH 8.0, 150 mM ammonium sulfate, 10% glycerol, 2 mM DTT, 1 mM EDTA) supplemented with protease inhibitor cocktail for fungi (Sigma-Aldrich). Whole-cell protein lysates from transfected HEK 293 cells were extracted using RIPA buffer (1× PBS, 1% Nonidet P-40, 0.5% sodium deoxycholate, 0.1% SDS) supplemented with a cocktail of protease inhibitors (Complete; Roche Molecular Biochemicals). All lysates were quantified using the Bradford method (Bio-Rad, Hercules, CA).

Forty micrograms of total protein were resolved on 10% SDS–PAGE gel and transferred to a nitrocellulose membrane (Protran 0.2-μm pore size; Schleicher & Schuell, Keene, NH). The membranes were blocked with 5% milk in TBST (50 mM Tris–HCl pH 7.4, 150 mM NaCl, 0.5% Tween-20) at 4°C overnight. Blots were incubated with primary antibody (1:500; Santa Cruz Biotechnology) for 1 h at 25°C and then washed three times with TBST. Secondary antibody conjugated with HRP (1:5000; Jackson Immunoresearch, West Grove, PA) was incubated for 45 min at 25°C. Visualization was carried out with enhanced chemiluminescence (ECL, Amersham Pharmacia Biotech, Piscataway, NJ).

Protein modeling

The hypothetical structures for EYA1 and its mutations were created using Swiss-Pdb Viewer (GlaxoSmithKline, www.expasy.org/spdbv). Structure optimization and modifications were made using Sybyl software (Tripos Associates, St. Louis, MO).

RESULTS

Novel Eya4 isoforms

We identified several tissue-specific *Eya4* isoforms by RT-PCR and verified results by sequencing of multiple clones. Although many of these splice variants have been reported previously (Borsani et al. 1999), two novel isoforms were seen isoform c-f and c-g, splice variants that exclude exon 6 (the inclusion or exclusion of exon 6 maintains the same open reading frame), and isoform d, a splice variant deleting the 5' 28 base pairs of exon 8. The putative protein generated by isoform d lacks the *Eya* homologous region and was cloned from an E11 murine embryonic cDNA library.

We demonstrated strong murine skeletal muscle expression of isoform a-g, which other investigators have reported as absent (Borsani et al. 1999). We also confirmed our earlier studies showing alternative splicing of exon 19 and exon 20 (isoforms f and g) in different tissues, with expression of isoform f in embryonic cells and isoform g in mature cells (Wayne et al. 2001). Isoforms b-f and c-f are expressed in fetal cochlea and b-g and c-g in adult cochlea (Fig. 1).

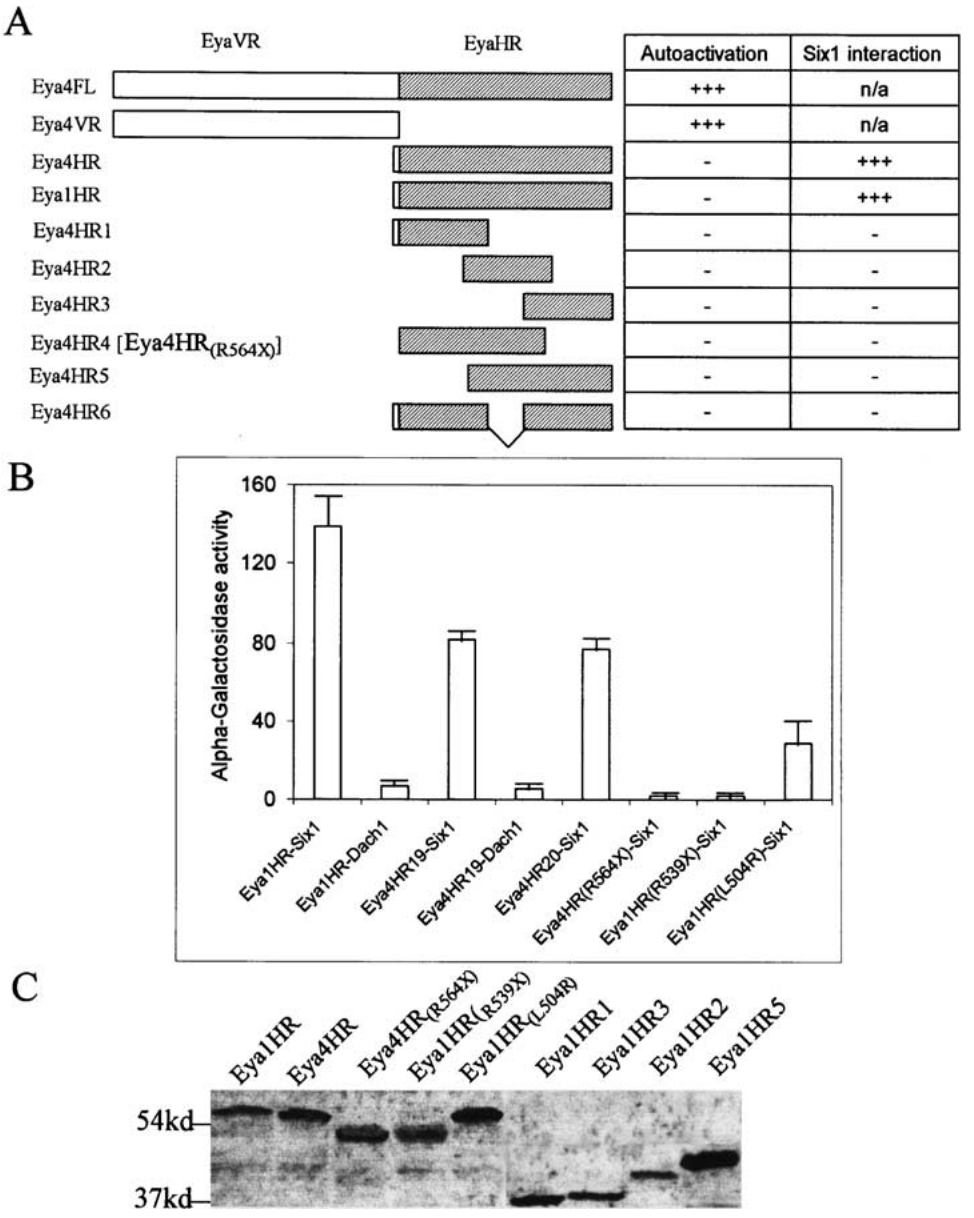

FIG. 2. Schematic of the Y2H bait constructs of *Eya4*. Constructs containing *EyaVR* autoactivated and were unsuitable as baits. None of the partial *EyaHR* constructs (*Eya4HR1–6*) generated proteins that interacted with Six1 (**A**). Interaction strengths were measured by assaying α-galactosidase activity after cotransformation of *Eya* (wild-type or mutant baits) with *Six1* (prey) or *Dach1* (prey). Nonsense mutant constructs of *Eya* did not interact with *Six1*, and with the L504R missense mutation of *Eya1*, interaction was reduced by 75 of expected levels. Neither *Eya1HR* nor *Eya4HR* baits interacted with *Dach1* prey (**B**). Immunoblotting of yeast extracts verified expression of wild-type and mutant proteins (**C**). FL, full length; VR, variable region; HR, homologous region.

Interaction between Eya1/Eya4 and Six1

We designed bait constructs of *Eya4* that included the entire coding region, only the *eyaVR*, and only the *eyaHR*. Although all constructs that contained the *eyaVR* autoactivated, *Eya4* constructs that contained only the *eyaHR* showed slight ''leakage'' of the *His* report gene that could be suppressed by adding 15 mM 3-AT (Fig. 2A). The *Eya1* constructs we designed showed a similar autoactivation profile.

To identify *Eya4* interacting partners, we used the *Eya4HR* construct as bait against an otic vesicle prey library (pGADT7; E10.5) in a Y2H mating screen. Mating efficiency was 2.5% and total screenable diploids were 1.6×10^7. One hundred sixty-five *Ade/His/MEL1* positive preys were rescued and subjected to second-round screening to eliminate (a) autoactivating prey by single transformation and (b) false positives by reintroducing one-by-one prey and *Eya4HR* bait. After second-round screening, three positive clones were identified that encoded the Six1 protein,

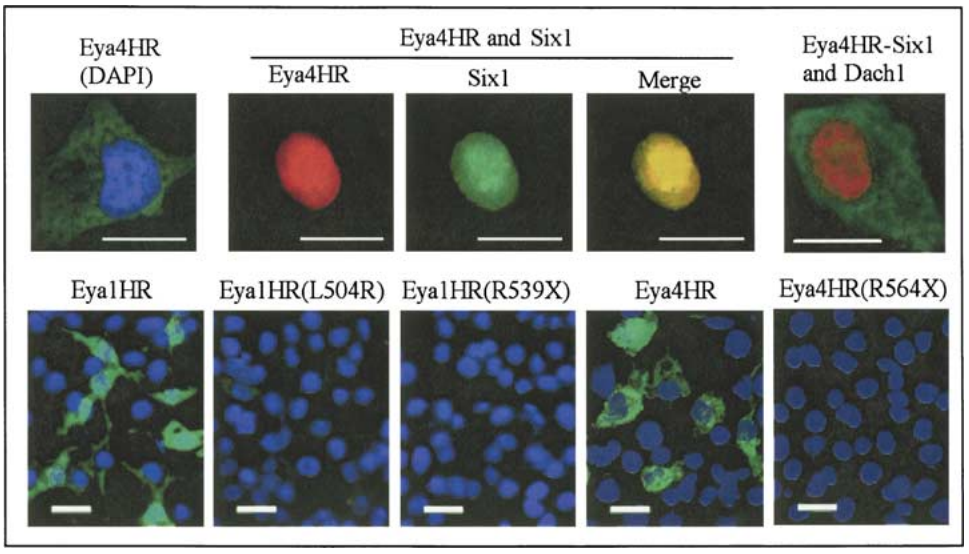

FIG. 3. Subcellular localization and translocation of wild-type and mutant Eya proteins in Cos-7 cells. Top row: Single transfection of c-myc-tagged *Eya4HR* shows cytoplasmic localization of the translated protein (green; blue, DAPI staining of the nucleus). Cotransfection of c-myc-tagged *Eya4HR* with HA-tagged *Six1* results in nuclear translocation of the Eya4HR/Six1 protein complex (EyaHR, red; Six1, green), as the merged image (yellow) shows. Coexpression of Eya4HR, Six1, and Dach1 shows flag-tagged Dach1 (green) is not recruited with the Eya4HR/Six1 protein complex into the nucleus (Eya4HR, red) (scale bars, 10 μm). Bottom row: Wild-type Eya1HR and Eya4HR proteins localize to the cytoplasm. Translation of the $Eya1HR_{L504R}$ bait construct is markedly reduced and translation of the $Eya1HR_{R539X}$ and $Eya4HR_{R564X}$ bait constructs is essentially nonexistent.

but other *Six* or *Dach* homologs were not identified. We verified the presence of *Dach1* in the otic vesicle prey library by PCR, although its expression was weaker than *Six1* (data not shown).

We evaluated α-galactosidase activities of the *MEL1* reporter gene after cotransformation of yeast AH109 with *Eya1HR/Six1* and *Eya4HR/Six1* and documented *in vivo* interaction of both Eya1HR and Eya4HR proteins with Six1. Of the two interactions, Eya1HR/Six1 was stronger (Fig. 2B). The interaction of the different Eya4 isoforms ($Eya4HR_{Ex19}$ and $Eya4HR_{Ex20}$) with Six1 was comparable. We tested but could not demonstrate a direct interaction of Eya1HR or Eya4HR protein with Dach1 using our Y2H system (Fig. 2B).

EyaHR and function

To determine the impact of the DFNA10-causing human EYA4 (R587X) mutation, we generated an $EYA4HR_{R564X}$ construct with mutation 2200CGA> → TGA (mouse Eya4 (R564X) [NP_034297] corresponding to human EYA4[NP_004091]). This construct generates a truncated protein missing the 53 carboxy-terminal amino acids of Eya4. Using our Y2H system, we were unable to demonstrate an interaction between $Eya4HR_{R564X}$ protein and Six1 (Fig. 2B). To investigate whether this finding was Eya4 specific, we generated a mutant bait construct of *Eya1HR* that contained the corresponding amino acid change (mouse Eya1 (R539X) [NP_034294]). This truncated protein also did not interact with Six1. Expression of both mutant Eya proteins was demonstrable in our Y2H system (Fig. 2C).

To determine whether a BOR-causing missense mutation abrogates the Six1 interaction, we next generated an $Eya1HR_{L504R}$ bait construct (mouse Eya1 (L504R) [NP_034294] corresponding to human (EYA1 (L472) [NP_742057]) as this mutation causes BOR syndrome with typical phenotypic features (Argiriadi et al. 1999). Using the Y2H system, we found that although the interaction between $Eya1HR_{L504R}$ protein and Six1 was not totally abolished, it was significantly reduced (Fig. 2B). As truncated EyaHR (loss of a small portion of the carboxy-terminus) did not interact with Six1, we sought to determine the requisite portion of the EyaHR protein for Six1 interaction by generating and testing several *Eya4HR* truncated constructs (*EyaHR1–6*; Fig. 2A). None was found to interact with Six1 (data not shown), although these mutant proteins were expressed (Fig. 2C).

Colocalization studies

We studied Eya localization in mammalian cells by immunofluorescence staining. Forty-eight hours after transfection, c-myc-tagged Eya4HR protein could be demonstrated in the cytoplasm, and after coexpression of HA-tagged *Six1*, it was translocated to the nucleus (Fig. 3). Flag-tagged Dach1 was localized in the cytoplasm and, when expressed with Six1 and

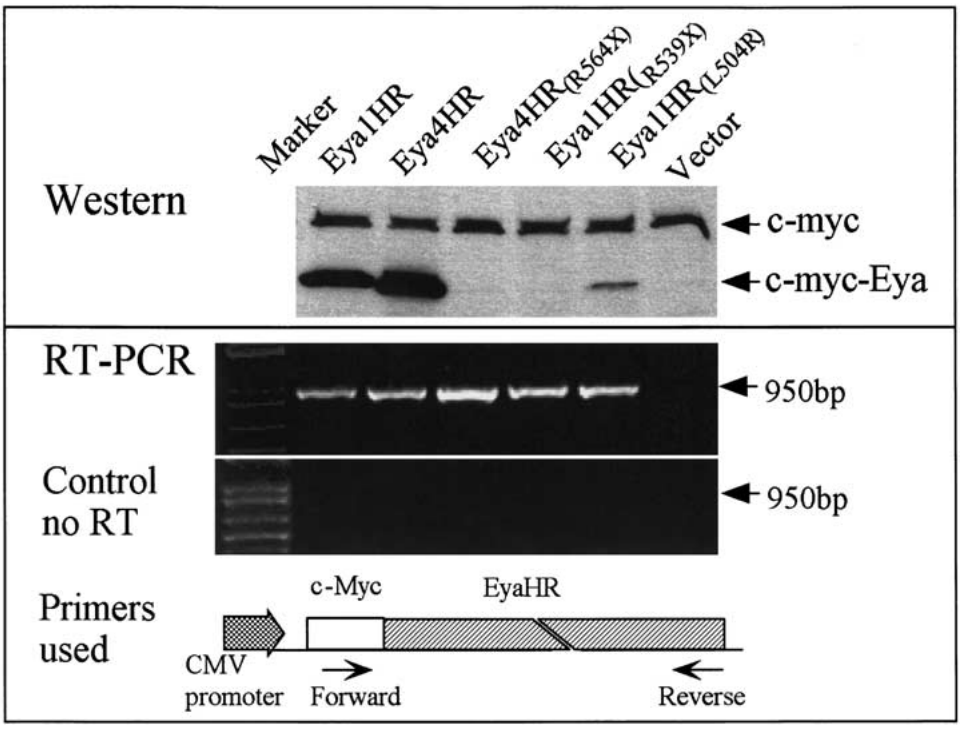

FIG. 4. Top row: Rapid degradation of mutant Eya protein after translation is apparent by immunoblotting 4 h after transfection (detection—primary antibody: mouse anti-c-myc antibody; secondary antibody: HRP-conjugated goat anti-mouse antibody). Bottom row: A parallel RT-PCR assay on total RNA extracted from HEK293 cells transfected with *Eya* constructs (wild-type and mutant) shows robust amplification of both wild-type and mutant tagged *Eya1HR* and *Eya4HR* mRNA using primers specific for the expressed fusion protein, while in the control (no RT), no amplification is seen.

Eya4HR, did not colocalize with the Eya4HR/Six1 protein complex (Fig. 3). When we tested c-myc-tagged *Eya1HR*, we confirmed reports demonstrating localization of Eya1HR protein to the cytoplasm with nuclear translocation when coexpressed with Six1 protein (data not shown) (Buller et al. 2001).

$Eya4HR_{R564X}$ and $Eya1HR_{R539X}$ proteins could not be demonstrated in transfected HEK 293 cells (Fig. 3). These results were confirmed with several independent clones and transfections and replicated using several other truncated constructs of *Eya4HR*. We also noted only very low fluorescence intensity of the translated protein using the BOR-causing $Eya1HR_{L504R}$ missense construct as compared to normal constructs (Fig. 3).

Mutant protein degradation

Translation of *EyaHR* mutant constructs containing nonsense mutations could not be demonstrated in transfected cells by immunoblot analysis. While we could detect wild-type c-myc-tagged Eya1HR and Eya4HR proteins as early as 4 h post-transfection, $Eya4HR_{R564X}$ and $Eya1HR_{R539X}$ proteins could not be detected at 4 or 16 h post-transfection. $Eya1HR_{L504R}$ protein was detectable as a very weak band (Fig. 4). Levels of tagged mRNA from wild-type constructs and mutant constructs showed comparable expression intensities using primers specific for the fusion proteins (Fig. 4).

Haploinsufficiency causes the BOR and DFNA10 phenotypes

As mutations in *EyaHR* appeared to be associated with rapid protein degradation, we sought to determine whether an *EyaHR* truncated mutant has a dominant-negative effect on a wild-type allele. We designed two dual *Eya* constructs, one containing two wild-type *EyaHR* (one with a c-myc tag and one with an HA tag) and one containing wild-type c-myc-tagged *EyaHR* and HA-tagged $EyaHR_{R564X}$. Transfection efficiency with both dual constructs was identical but in the mutant-containing construct only the c-myc-tagged protein was identified. To verify this result, we used Western blotting to semi-quantitate c-myc-tagged and HA-tagged Eya4HR proteins and could not demonstrate mutant HA-tagged Eya4HR (Fig. 5). These findings exclude a dominant-negative effect as the cause of BOR syndrome or DFNA10.

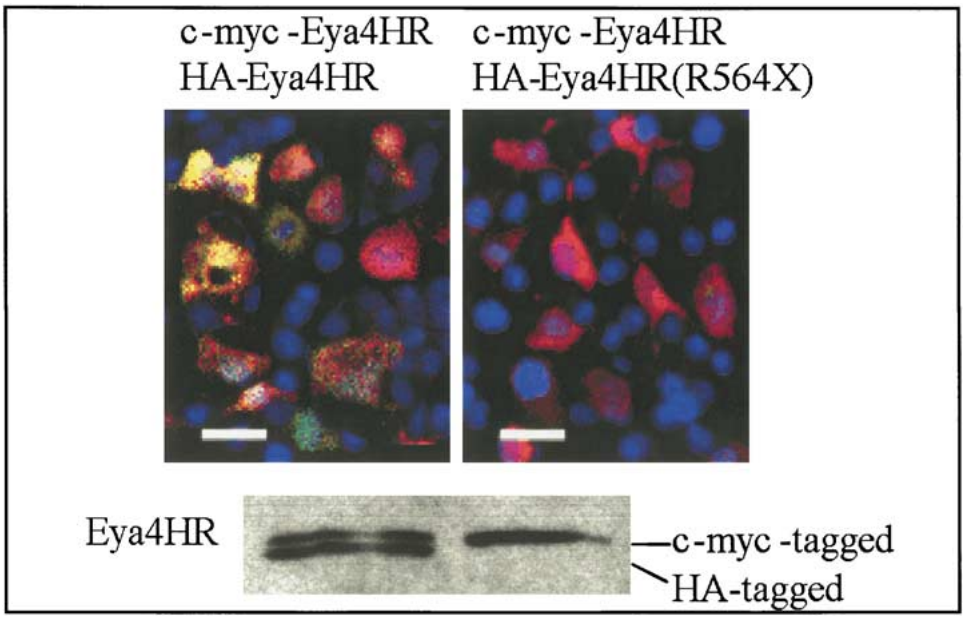

FIG. 5. Top row: pBudCE4.1 containing two wild-type *EyaHR* inserts (one with a c-myc tag and one with an HA tag) show good translation of both proteins (yellow) in most cells. When the HA-tagged wild-type *EyaHR* insert is replaced with HA-tagged *Eya4HR*$_{R564X}$, although transfection efficiency remains similar, the HA-tagged Eya4HR$_{R564X}$ protein cannot be identified (scale bars, 20 μm). Bottom row: Cell extracts subjected to immunoblotting with two primary monoclonal antibodies against c-myc tag (9E10) and HA-tag (F-7) show no translation of the mutant construct (right).

Molecular modeling

Hypothetical models for Eya1, Eya1$_{L504R}$, and Eya1$_{R539X}$ proteins were created using Swiss–Pdb-Viewer (GlaxoSmithKline, www.expasy.org/spdbv) to thread the amino acid sequence of Eya1 onto the known structure of epoxide hydrolase (www.pdb.org PDB ID: 1CQZ), which was a match for Eya1 in the NCBI conserved domain database (www.ncbi.nlm.nih.gov/Structure/cdd/cdd.shtml) (Abdelhak et al. 1997a). Compared with the Eya1$_{R539X}$ protein, the model of Eya1$_{L504R}$ shows a change secondary to the point mutation that moves the carboxy-terminal section truncated in Eya1$_{R539X}$ to the other side of the molecule, thereby causing similar alterations in structure (Fig. 6).

DISCUSSION

The mechanism by which a mutation produces a dominant phenotype is seldom intuitively clear, but as a general rule these types of mutations cause either loss or gain of function. Loss of function typically implies haploinsufficiency through reduced gene dosage, expression, or protein activity, while gain of function implies increased gene dosage, altered mRNA expression, increased or abnormal protein activity, or dominant-negative effects (Wilkie 1994). Particularly vulnerable to haploinsufficiency are regulatory genes working close to threshold levels in specific tissues. Examples include *PAX3*, which is responsible for Waardenburg syndrome Type 1 (Tassabehji et al. 1995), and *SOX9*, a cause of campomelic dysplasia (Sock et al. 2001). Based on our data, *EYA1* and *EYA4* can be added to this list.

Using the Y2H system, we confirmed the reported interaction of Eya1HR/Six1 (Buller et al. 2001) and showed that Six1 protein also interacts, albeit more weakly, with Eya4HR protein. We identified the Eya4HR/Six1 protein interaction by screening an E10.5 otic vesicle prey library and found that both Eya4 isoforms (*Eya4HR*$_{Ex19}$ and *Eya4HR*$_{Ex20}$) have comparable affinity for Six1, although only the exon 19-containing variant is present in the developing inner ear (Wayne et al. 2001). This functional redundancy of *Eya4* to *Eya1* with respect to *Six1* is consistent with the absence of a congenital phenotype in persons with DFNA10 deafness (De Leenheer et al. 2001).

Other investigators have proposed an Eya1HR/Dach1 interaction (Chen et al. 1997), which we could not verify in our Y2H system. We were also unable to demonstrate direct binding of Eya4HR and Dach1 proteins and found that Dach1 did not colocalize with the Eya4HR/Six1 protein complex. Interestingly, an Eya1/Dach1 interaction has been demonstrated using a mammalian 2-hybrid system (Ozaki et al. 2002), suggesting that either the full-length protein or EyaVR is required to interact with Dach1, or that the interaction between Dach1 and EyaHR re-

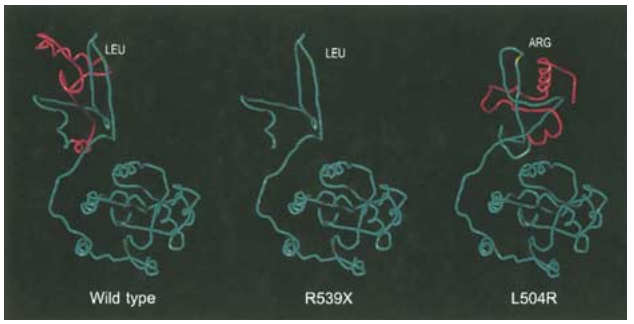

FIG. 6. The likely structures (backbone only) for Eya1, $Eya1_{R539X}$, and $Eya1_{L504R}$ proteins are shown. In purple is the section of the protein that is truncated in $Eya1_{R539X}$, in green is the site of the point mutation, which is depicted as yellow in $Eya1_{L504R}$. The hypothetical change due to the point mutation moves the section truncated in $Eya1_{R539X}$ to the other side of the molecule in $Eya1_{L504R}$.

TABLE 2

Correlation between BOR syndrome phenotypes and genotypes

	Phenotype	
Genotype	*Severe*	*Mild*
Truncating mutations	19	6
Nontruncating mutations	8	2

$p = 0.799$.

quires a third protein that is not expressed in the experimental systems we used.

By generating truncating mutant constructs (*Eya4HR*$_{R564X}$ and *Eya1HR*$_{R539X}$), we abolished the interaction of Eya proteins with Six1. Based on this finding, we hypothesized that a Six1 domain could be defined, but although we made numerous partial constructs of the EyaHR domain that were expressed, we were unable to identify a Six1 binding site. Based on these data, we believe the Eya/Six protein–protein interaction is dependent on the juxtaposition of several distant amino acids of Eya brought in proximity by the three-dimensional conformation of the homologous region. In support of this hypothesis, we found that the missense construct *Eya1HR*$_{L504R}$ also had significantly reduced Six1 affinity, presumably on the basis of a conformational change (Fig. 6).

Translation of the two *EyaHR* nonsense-containing mutant constructs could not be demonstrated in transfected cells by immunoblot analysis and the missense $Eya1HR_{L504R}$ protein was detectable only as a very weak band (Fig. 4). Because levels of tagged mRNA from wild-type and mutant constructs showed comparable expression intensities using a pair of tagged gene-specific primers (Fig. 4), we believe that mutant proteins are rapidly degraded and that haploinsufficiency causes the BOR and DFNA10 phenotypes. Additional *in vitro* support for this hypothesis comes from studies using dual *EyaHR* constructs. While we could demonstrate equivalent transfection efficiency, we could not identify the HA-tagged $Eya1HR_{L504R}$ mutant protein either by immunostaining or by Western blotting (Fig. 5).

The BOR-typical L504R mutation represents a decrease in hydrophobicity and an increase in electrostatic charge and size of the amino acid side chain at position 504. These changes affect the interaction of the mutation site with neighboring amino acids and the surrounding environment, and on this basis the resultant three-dimensional protein structure of $Eya1_{L504R}$ appears significantly altered. Major differences in protein conformation are also predicted by trypsin digestion studies that show a low sensitivity to but distinct pattern of digestion of the $Eya1_{L504R}$ mutant protein compared with wild-type protein (Ozaki et al. 2002). Similarities in the protein structure of $Eya1_{R539X}$ and $Eya1_{L504R}$ are consistent with the rapid degradation we observed (Fig. 6).

Haploinsufficiency as the cause of BOR syndrome is supported by genotype–phenotype studies based on the different allele variants of *EYA1* in persons segregating a BOR phenotype. Notably included in this list of 51 different mutations are 23 frameshift or nonsense mutations, 8 missense mutations, 9 splice site mutations, and 11 complex mutations involving large deletions or chromosomal rearrangements (www.medicine uiowa.edu/pendredandbor). Although Abdelhak et al. (1997a) hypothesized that the majority of BOR-causing mutations cluster in the eyaHR, they are in fact randomly scattered throughout the gene, with complex rearrangements involving every exon and point mutations and small insertions/deletions occurring in every exon except for exons 1–3.

The clinical phenotype that results from these mutations variably affects the branchial arch system, inner and middle ears, and kidneys. If we define classical BOR syndrome as the presence of at least three of these cardinal features (Chen et al. 1995) and define subgroup genotypes as inactivating or noninactivating (inactivating—splice site mutations, insertions, nonsense mutations, and duplications and deletions of more than 3 bp; noninactivating mutations—missense mutations and 3-bp deletions), we can compare phenotype with genotype to show that inactivating mutations are not associated with a more severe clinical disease spectrum ($p = 0.799$; Table 2). A similar comparative study with DFNA10-causing *EYA4* mutations is not possible as only three families have been reported to segregate deafness at this locus. The responsible mutations include a nonsense mutation and two frame shift-causing deletions, all of

which affect the eyaHR (Wayne et al. 2001; Pfister et al. 2002).

In conclusion, our data suggest that the functional integrity of *EyaHR* depends on its three-dimensional conformation. Although autoactivation of *Eya4FL* and *EyaVR* constructs precluded their use as bait in our Y2H system, we studied multiple *EyaHR* constructs. Both Eya1HR and Eya4HR proteins bind Six1, with subsequent nuclear translocation. Six1, in turn, can bind to specific DNA promoters, with an affinity that may be modulated by EyaVR. We observed no EyaHR–Six1 interaction with Dach1. Furthermore, in our Y2H system the EyaHR mutant proteins we studied did not interact with Six1, and in the mammalian system were rapidly degraded. In concurrence with clinical data, our findings imply that haploinsufficiency is the basis for the BOR and DFNA10 phenotypes.

ACKNOWLEDGMENTS

This research was supported in part by NIH grant R01-DC03544 (RJHS).

REFERENCES

Abdelhak S, Kalatzis V, Heilig R, Compain S, Samson D, Vincent C, Levi–Acobas F, Cruaud C, Le Merrer M, Mathieu M, Konig R, Vigneron J, Weissenbach J, Petit C, Weil D. Clustering of mutations responsible for Branchio-Oto-Renal (BOR) syndrome in the eyes absent homologous region (eyaHR) of EYA1. Hum. Mot. Genet. 6:2247–2255, 1997a.

Abdelhak S, Kalatzis V, Heilig R, Compain S, Samson D, Vincent C, Weil D, Cruaud C, Sahly I, Leibovici M, Bitner–Glindzicz M, Francis M, Lacombe D, Vigneron J, Charachon R, Boven K, Bedbeder P, Van Regemorter N, Weissenbach J, Petit C. A human homologue of the *Drosphila* eyes absent gene underlies branchio-oto-renal (BOR) syndrome and identifies a novel gene family. Nat. Genet. 15:157–164, 1997b.

Argiriadi MA, Morisseau C, Hammock BD, Christianson DW. Detoxification of environmental mutagens and carcinogens: structure-based mechanism and evolution of liver epoxide hydrolase. Proc. Natl. Acad. Sci. USA 96:10637–10642, 1999.

Bonini N, Leiserson W, Benxer S. The eyes absent gene: genetic control of cell survival and differentiation in the developing *Drosophila* eye. Cell 72:971–982, 1993.

Bonini NM, Quang T, Gray–Board GL, Warrick JM. The *Drosophila eyes absent* gene directs ectopic eye formation in a pathway conserved between flies and vertebrates. Development 124:4819–4826, 1997.

Borsani G, Degrani A, Ballabio A, Bulfone A, Bernard L, Banfi S, Gattuso C, Mariani M, Dixon M, Donnai D, Metcalfe K, Winter R, Robertson M, Axton R, Brown A, Van Heyningen V, Hanson I. Eya4, a novel vertebrate gene related to *Drosophila* eyes absent. Hum. Mol. Genet. 8:11–23, 1999.

Buller C, Xu X, Marquis V, Schwanke R, Xu P-X. Molecular effects of Eya1 domain mutations causing organ defects in BOR syndrome. Hum. Mol. Genet. 10:2775–2781, 2001.

Chen AH, Francis M, Ni L, Cremers CWRJ, Kimberling WJ, Sato Y, Phelps PD, Bellman SC, Wagner MJ, Pembrey M, Smith RJH. Phenotypic manifestations of branchiootorenal syndrome. Am. J. Med. Genet. 58:365–370, 1995.

Chen R, Amoui M, Zhang Z, Mardon G. Dachshund and eyes absent proteins form a complex and function synergistically to induce ectopic eye development in *Drosophila*. Cell 91:893–903, 1997.

De Leenheer EMR, Huygen PLM, Wayne S, Smith RJH, Cremers CWRJ. The DFNA10 phenotype. Ann. Otol. Rhinol. Laryngol. 110:861–866, 2001.

Heanue TA, Reshef R, Davis RJ, Mardon G, Oliver G, Tomarev S, Lassar AB, Tabin CJ. Synergistic regulation of vertebrate muscle development by Dach2, Eya2, and Six1, homologs of genes required for *Drosphila* eye formation. Genes Dev. 13:3231–3243, 1999.

Ohto H, Kamada S, Tago K, Tominaga SI, Ozaki H, Sato S, Kawakami K. Cooperation of Six and Eya in activation of their target genes through nuclear translocation of Eya. Mol. Cell. Biol. 19:6815–6824, 1999.

Ozaki H, Watanabe Y, Ikeda K, Kawakami K. Impaired interactions between mouse Eya1 harboring mutation found in patients with branchio-oto-renal syndrome and Six, Dach, and G proteins. J. Hum. Genet. 47:107–116, 2002.

Pfister M, Toth T, Thiele H, Haack B, Blin N, Zenner HP, Sziklai I, Mumberg P, Kupka S. A 4-bp insertion in the eya-homologous region (eyaHR) of EYA4 causes hearing impairment in a Hungarian family linked to DFNA10. Mol. Med. 8:607–611, 2002.

Pignoni F, Hu B, Zavitz KH, Xiao J, Garrity PA, Zipursky SL. The eye-specification proteins So and Eya from a complex and regulate multiple steps in *Drosophila* eye development. Cell 91:881–891, 1997.

Singh MV, Weil AP. A method for plasmid purification directly from yeast. Anal. Biochem. 307:13–17, 2002.

Sock E, Pagon RA, Keymolen K, Lissens W, Wegner M, Scherer G. Loss of DNA-dependent dimerization of the transcription factor SOX9 as a cause for campomelic dysplasia. Hum. Mol. Genet. 12:1439–1447, 2003.

Tassabehji M, Newton VE, Liu XZ, Brady A, Donnai D, Krajewska–Walasek M, Murday V, Norman A, Obersztyn E, Reardon W. The mutational spectrum in Waardenburg syndrome. Hum. Mol. Genet. 4:2131–2137, 1995.

Wayne S, Robertson NG, Declau F, Chen N, Verhoeven K, Prasad S, Tranebjarg L, Morton C, Ryan AF, Van Camp G, Smith RJH. Mutations in the transcriptional activator EYA4 cause late-onset deafness at the DFNA10 locus. Hum. Mol. Genet. 10:195–200, 2001.

Wilkie AOM. The molecular basis of genetic dominance. J. Med. Genet. 31:89–98, 1994.

Xu P-X, Woo I, Her H, Beier D, Maas R. Mouse Eya homologues of the *Drosophila eyes absent* gene require Pax6 for expression in cranial placodes. Development 124:219–231, 1997.

Zimmerman JE, Bui QT, Steingrimsson E, Nagle DL, Fu W, Genin A, Spinner NB, Copeland NG, Jenkins NA, Bucan M, Bonini NM. Cloning and characterization of two vertebrate homologs of the Drosophila eyes absent gene. Gen. Res. 7:128–141, 1997.